drones

MDPI

Article

Design and Modeling of an Experimental ROV with Six Degrees of Freedom

Aleksey Kabanov *, Vadim Kramar and Igor Ermakov

Robotics and Intelligent Control Systems Laboratory, Sevastopol State University, 299053 Sevastopol, Russia; kramarv@mail.ru (V.K.); ErmakovIgorROV@gmail.com (I.E.)
* Correspondence: kabanovaleksey@gmail.com

Abstract: With the development of underwater technology, it is important to develop a wide range of autonomous and remotely operated underwater vehicles for various tasks. Depending on the problem that needs to be solved, vehicles will have different designs and dimensions, while the issues surrounding reduced costs and increasing the functionality of vehicles are relevant. This article discusses the development of inspection class experimental remotely operated vehicles (ROVs) for performing coastal underwater inspection operations, with a smaller number of thrusters, but having the same functional capabilities in terms of controllability (as vehicles with traditionally-shaped layouts). The proposed design provides controllability of the vehicle in six degrees of freedom, using six thrusters. In classical design vehicles, such controllability is usually achieved using eight thrusters. The proposed design of the ROV is described; the mathematical model, the results of modeling, and experimental tests of the developed ROVs are shown.

Keywords: remotely operated vehicle; underwater robot; kinematic model; vehicle maneuverability

Citation: Kabanov, A.; Kramar, V.; Ermakov, I. Design and Modeling of an Experimental ROV with Six Degrees of Freedom. *Drones* **2021**, *5*, 113. https://doi.org/10.3390/drones5040113

Academic Editors: Andrey V. Savkin and Kooktae Lee

Received: 31 August 2021
Accepted: 1 October 2021
Published: 8 October 2021

1. Introduction

With the development of underwater technology, it is important to develop a wide range of autonomous and remotely operated underwater vehicles for various tasks. Depending on the problem that needs to be solved, vehicles will have different designs and dimensions. Remotely operated underwater vehicles (ROV) are controlled by one or more operators from the vessel, and are connected to the vessel by a cable, through which control commands and the power supply are supplied to the vehicle. This type of underwater vehicle allows one to solve a wide range of tasks: bottom mapping, inspection work, rescue operations, extraction of objects from the bottom, work to ensure oil and gas complex objects (drilling support, inspection of gas pipeline routes, inspection of structures for breakdowns, performing operations with valves and valves), scientific applications, support for diving operations, work to maintain fish farms, archaeological surveys, inspection of urban communications, inspection of ships, etc. The tasks to be solved are constantly expanding, and the fleet of underwater robots is growing rapidly [1–10]. Working with the robots is much cheaper than expensive diving work, despite the fact that the initial investment is quite large, although working with the robots cannot replace the entire range of diving work.

As a rule, a standard underwater vehicle has the following equipment [8]:

- Engines (from three to ten or more);
- Pressure sensor;
- Compass or gyrocompass for orientation in space;
- Video cameras;
- Lighting equipment;
- Manipulator;
- All-round sonar;
- Beacon transponder hydroacoustic navigation system (HANS).

An inspection class underwater vehicles often lacks a manipulator and sonar. In addition, there can be other simplifications.

Some of the most important requirements for the development of inspection class underwater vehicles are to increase their maneuverability and reduce energy consumption and costs. These tasks are still critical, despite the large number of publications and developments on this topic.

The authors of [2] conducted a review of underwater robots, in terms of morphological characteristics and the layout of the propulsion devices. The geometric shapes depend on many factors. First, the shape is influenced by the distribution of internal electronic devices, sensors, motors, drags, etc. Moreover, the degrees of freedom of the robots must be taken into account separately, since they depend on the arrangement of thrusters in the structure. One of the most common shapes of underwater robots is the torpedo-like cylindrical shape. This shape is more often used for autonomous vehicles; it allows underwater robots to move at high speeds along the horizontal axis and descend diagonally using rudders. There are other types of underwater robots that have the shape of a torpedo, but instead of rudders, they use more thrusters. An example is the robot Nessie (the sixth version [11]). The Nessie robot has six thrusters: two for lateral movement, two for vertical and pitch movement, and two for forward and yaw control.

In addition to cylindrical shape, some recent studies have focused on the use of fully symmetrical shapes for underwater robots, which have advantages over traditional shapes due to symmetry. An example is the spherical underwater robot (SUR), the design of which was developed in 2012 [12], as well as its modifications—SUR-II and SUR-III [13,14]. For example, the SUR-III propulsion system consists of four-vector jet thrusters, eight steering motors, and a circular support frame. Four jet thrusters are located around the circumference at a distance of $\frac{1}{4}$ from each other and are fixed on an annular support frame. The vector jet can rotate in the X–Z plane and the Y–Z plane. In this way, the four forces can be combined to realize underwater movements, such as lift, splash, and yaw.

ROVs, in the form of rectangular frames, on which the main components of the robots are attached (for example, sealed boxes, lanterns, thrusters, and other devices), have become widespread. The frame structure allows easy access to the robot components. Examples of such robots are CISCREA [15] and BlueROV2 [16]. The CISCREA robot had six thrusters: four of them were outside the longitudinal axis of the robot, which gave it better torque, greater longitudinal stability, and better movement. The other two thrusters were located on the horizontal axis and had to control the depth. Blue Robotics BlueROV2 robot has eight thrusters: four in a vertical plane, four in a horizontal plane. This allows the robot to move in all six degrees of freedom and gives the advantage of a more vertical thrust.

The location and number of the thrusters depend on how many degrees of freedom the robot will have, which is an important property for inspection vehicles. There are designs in which, to achieve all degrees of freedom, either a larger number of fixed thrusters are used, or thrusters with rotary drives to change the direction of the thrust force. Analyses of the structures of underwater robots showed that structures and designs with four rotary thrusters provide five degrees of freedom in comparison to structures where six fixed thrusters are required to achieve five degrees of freedom. At the same time, to achieve all six degrees of freedom in underwater robots, eight fixed thrusters or five thrusters with two rotary drives are used to change the direction of the thrust force. Although it is clear that to achieve six degrees of freedom, there should be at least six fixed thrusters [9].

The purpose of this work was to develop a new design of an inspection-class ROV, with a minimal number of thrusters to achieve controllability in six degrees of freedom. The advantage of the proposed design of the robot is that with six fixed thrusters, six degrees of freedom are provided. Authors from ground mobile robotics borrowed the idea of the proposed new arrangement of thrusters when three degrees of freedom were achieved in the designs of three-wheeled mobile robots with omnidirectional wheels. The rest of the article reveals the details of the proposed new design of the underwater vehicle and describes the main elements and components of the created prototype. Special attention

is paid to the development of a mathematical model of the movement of the created underwater robot and the simulation and experimental tests results. At the end of the article, a discussion of the results, the advantages and disadvantages of using the proposed new design, the arrangement of the underwater robot thrusters, a plan for future research, and unsolved problems, are presented.

2. Materials and Methods

2.1. Design Rationale

While implementing this project, we decided to create a new configuration of the ROV with the so-called Y-arrangement of thrusters.

According to the proposed arrangement, there are three thrusters with a thrust in the horizontal plane and three thrusters with a thrust in the vertical plane. Thrusters with horizontal thrusts are located in one plane at a distance from the center of rotation of the vehicle, in a circle, with a step of 120 degrees relative to the vertical axis. In this case, the vectors of the horizontal thrust of the thrusters are located tangentially to the indicated circle. Thus, this group of thrusters provides controlled linear movement in the horizontal plane along the two degrees of freedom and rotational movement relative to the vertical axis of the vehicle.

Thrusters with a thrust in the vertical plane are located similarly to a group of horizontal thrusters at a distance from the center of rotation of the vehicle in a circle with a step of 120 degrees relative to the vertical axis. Thus, this group of thrusters provides a controlled linear movement of the vehicle in the vertical plane and rotational movement relative to the longitudinal and transverse axes of the vehicle.

All thrusters in a complex manner allow achieving full controllability of the vehicle in degrees of freedom when using 6 thrusters, which is usually achieved with 8 thrusters in classic configurations.

The developed ROV is named SevROV. The arrangement of the SevROV thrusters is shown in Figure 1.

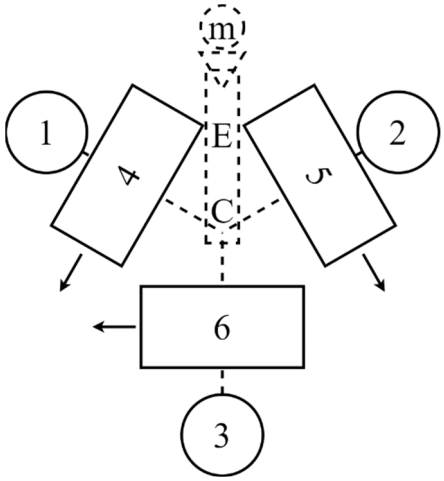

Figure 1. The arrangement of the SevROV thrusters.

Let us compare two popular 6-thruster (Figure 2a) and 8-thruster (Figure 2b) schemes of the ROV with the proposed one (Table 1). Because of using the proposed layout, we get lower thrusts in the horizontal directions compared to the classic 6-thruster layouts, by 11% in the lag and 32% in the marching direction. However, the vertical thrust becomes 33% larger when using the same thrusters. A decrease in the thrust leads to a decrease in the speed characteristics of the vehicle; however, in most cases of application, the speed qualities are not of paramount importance.

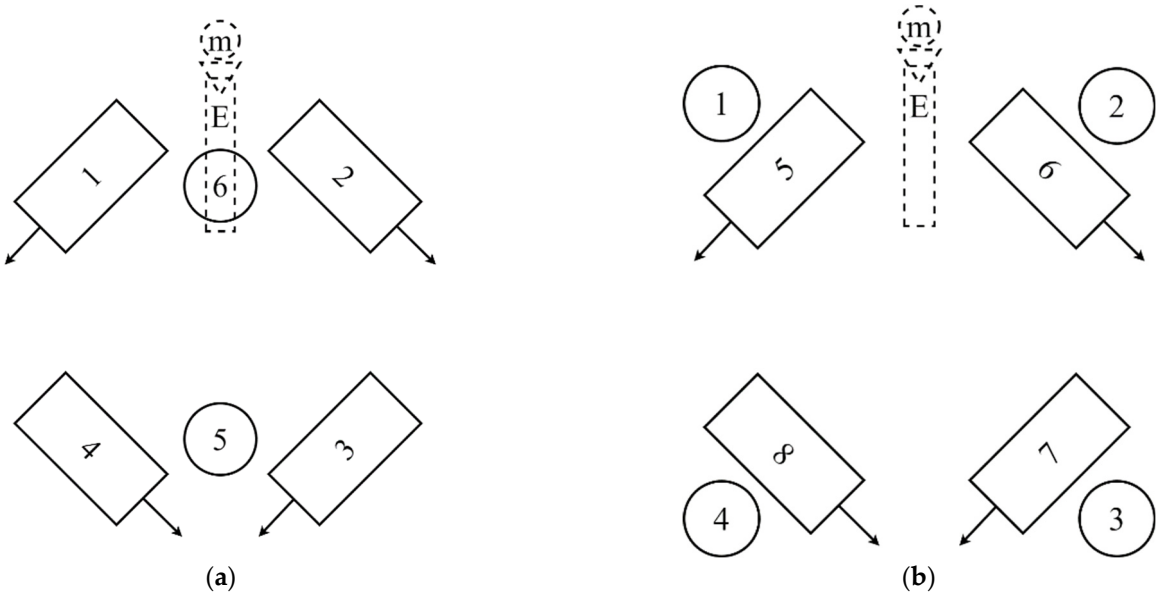

(**a**) (**b**)

Figure 2. (**a**) The 6-thruster arrangement scheme, (**b**) the 8-thruster arrangement scheme.

Table 1. Comparison of the thrust of various ROVs with Blue Robotics T100 thrusters.

Thrust	6 Thrusters Y-Frame	6 Thrusters Classical Frame	8 Thrusters Classical Frame
Forward, N	25.49	37.26	37.26
Lateral, N	33.34	37.26	37.26
Vertical, N	44.13	29.42	58.84

Classical thruster arrangement systems also use a vector-based approach, which in general makes the control and stabilization systems as complex as for the proposed scheme. The scheme we propose is more complicated, in that it has asymmetric force vectors when moving along some axes. However, by solving this complexity, one can get a more efficient system. Thus, in comparison with the classic 6-thruster scheme, we get an additional thruster for moving vertically and full controllability in the roll and pitch, which makes it possible to improve stabilization along these axes. Vertical movement and good stabilization make it possible to work with loads, and the location of the thrusters in our vehicle simplifies the work with objects placed in the front gripper. Thus, we have shown that SevROV can lift loads attached in front of the vehicle (on a manipulator) weighing 3 kg under water without loss of stability due to active stabilization.

2.2. Hardware and Software

A systematic approach was applied in the development of the SevROV prototype. Its use made it possible to divide the vehicle into many systems (subsystems), the development of which could go on independently. One advantage of the systematic approach is the simplicity in making changes to the final system, since, when making changes, we immediately know what subsystems it will affect and we do not need to make changes to the entire vehicle.

To investigate the effectiveness of the proposed thruster arrangement, we developed an experimental vehicle with a Y-arrangement of thrusters, called SevROV. This experimental vehicle contains several systems and subsystems:

- Propulsion system;
- Control system:
    - Navigation system;

- Computing module;
- Control software;

- Power supply and communication system:
  - Tether;
  - Ground power system;
  - Underwater power system;
  - Interconnection boards;
- Carrier system:
  - Frame;
  - Sealed housing for electronics;
  - Buoyancy and ballast;
- Payload:
  - Camera;
  - Manipulator.

2.2.1. Propulsion System

The propulsion system is one of the key systems in our research since it realizes the uniqueness of the vehicle.

The basis of this system consists of six Blue Robotics T100 thrusters, which have the following technical characteristics:

- Thrust—14.7 N in the forward direction and 11.77 N in the reverse direction;
- Dimensions—72 × 92 mm;
- Mass—0.075 kg;
- Electric power—up to 150 W when powered from 12 V DC;
- Supply voltage—12–24 V.

The thrusters are controlled using pulse width modulation (PWM) and special drivers that are part of each thruster.

2.2.2. Control System

The control system is the most important system of the vehicle and combines a computing module, a navigation module, and control software.

The key parts of the control system are computing modules: a Raspberry PI 3b + microcomputer and a ground station computer, which are connected using a tether. These components carry out all the calculations and allow one to control the ROV in the teleoperation mode. All automatics are included in the software for the microcontroller and are made in such a way that, if communication is lost, the ROV remains stable and does not lose its position. It also allows the implementation of various semi-automatic and autonomous control modes to simplify the operator's work.

The main idea behind creating the SevROV motion control software is flexibility. We have chosen one of the easiest ways to achieve this—to control the SevROV from a personal computer (PC). This allows us to make changes to the programs and settings of the robot and does not require changing the firmware of any computing module to make small changes. To program the robot, it is enough to simply connect to the Raspberry PI via SSH or VNC and change any part of the control system.

The software of the motion control system currently only implements a manual control mode of the robot. First, the Y-shaped arrangement of the thrusters requires complex control system settings and stability for operation in automatic mode. At the moment, it is possible to obtain acceptable system quality characteristics in the manual control mode.

The control system software consists of two programs: a client for a PC and a server for a Raspberry PI.

The client program works with a gamepad or joystick, an AVerMedia USB recorder, and SevROV over the UDP protocol. The only requirement that exists in the system is

that SevROV and the client PC must be on the same local network. This requirement is implemented using a router in the SCU.

The server program is a Python script without any user interface. It starts automatically when the Raspberry PI is loaded and waits for the client connection. After connecting from the client side, the server starts to send the telemetry and issues control commands. The server works with UDP, GPIO, I2C, and USB to control the SevROV. The stabilization subsystem works even if the client is not connected to the robot, so if there are problems with the connection, the vehicle will remain in a stable state.

On the server side of the software, a robot stabilization system is implemented, which works in conjunction with the navigation system. NavX 2 inertial navigation module allows one to receive data on angular and linear accelerations, speeds, and coordinates. The module's angular accuracy allows precise angular movements in roll, pitch, and yaw. Based on this module, an angular stabilization system is implemented, which greatly simplifies the work of the vehicle operator. The linear displacement accuracy of this inertial navigation system had a large cumulative error (1 m in 15 s), which makes it impossible to use it to determine the linear displacements and coordinates of the vehicle.

Another part of the stabilization system is depth stabilization, implemented using a depth sensor. The depth sensor is a pressure sensor, the depth values from which are obtained using simple calculations based on the density of the environment.

2.2.3. Power Supply and Communication System

This system is divided into communication and power supply subsystems.

The power supply of the vehicle occurs through a tether that connects the ground station with the underwater vehicle. The ground station houses DC/DC converters to power the Ethernet router and the vehicle. A 48 V DC converter with a power of 1000 W is used to power itself. Further, the power is supplied through the tether and is converted on the vehicle to 12 V. The increased voltage on the tether is made to reduce electrical losses associated with the resistance of the tether.

There are two 48 V–12 V DC converters on the vehicle, each with a power of 500 W. They are located outside the frame of the vehicle, for which additional sealing was carried out. Moreover, the location of the outside allows for better cooling of the converters under high load but complicates the connection.

SevROV electronic components consist of:

- Microcomputer Raspberry Pi—serves to convert control signals, send data to the base station, control all components of the robots;
- Power and signal routing boards;
- navX navigation sensor—serves to determine the angular coordinates of the device;
- Pressure sensor—serves to determine the depth of the device, is installed in the hole for the penetrator.

A system integration diagram (SID) of SevROV is shown in Figure 3.

The interconnection boards are used to connect all components of the electronic system of the device. They were developed using the EasyEDA open development system and then sent to a third party for production.

Inside the sealed electronics box, all power and signal lines are connected. For the implementation of connections and conversions, a printed circuit has been developed that routes all signals and allows one to easily connect and replace the components of the device. The board is shown in Figure 4.

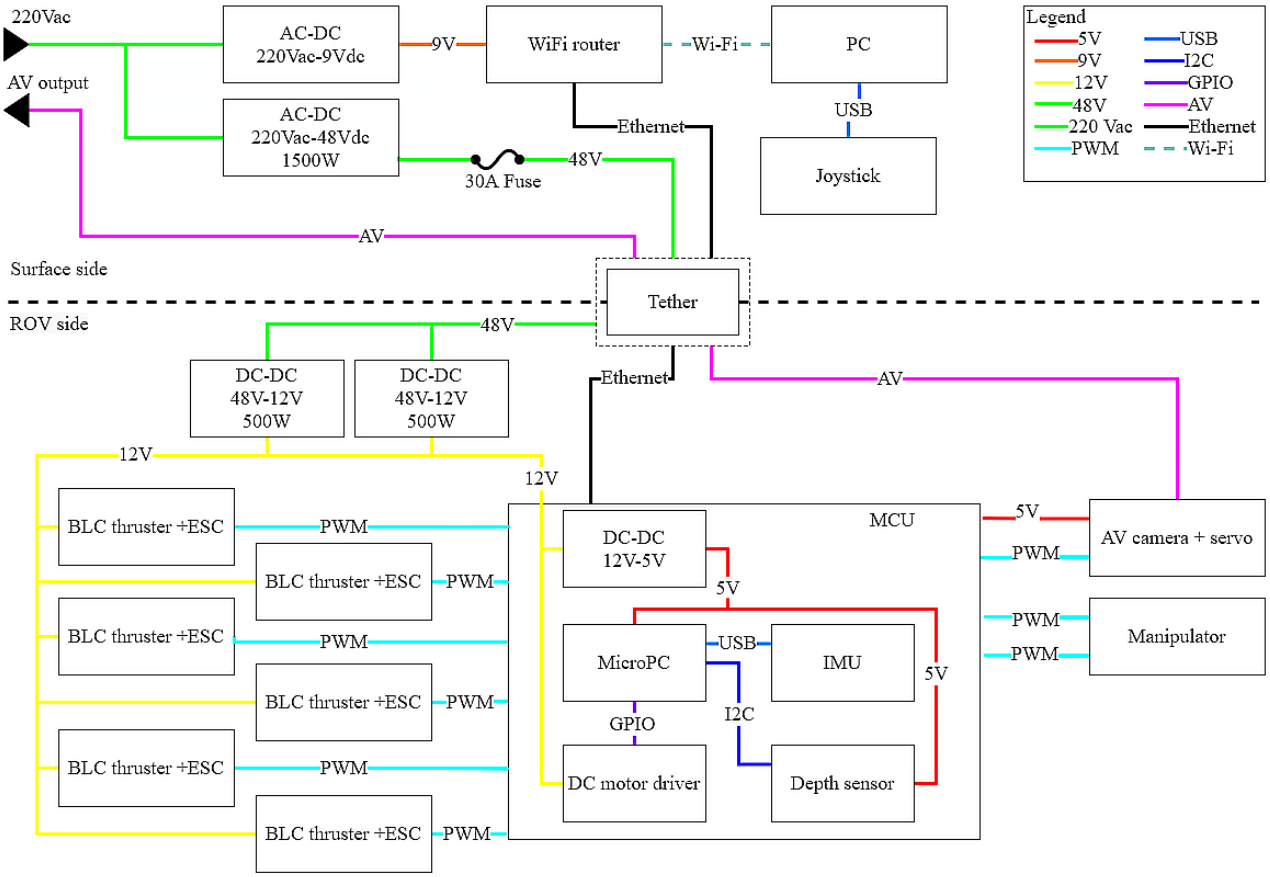

Figure 3. System integration diagram.

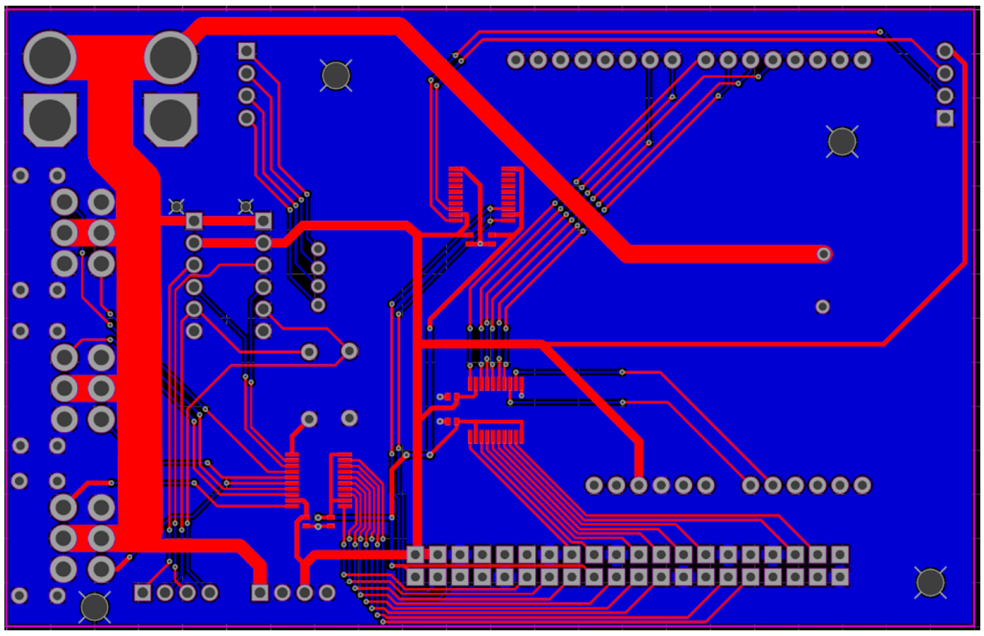

Figure 4. Design of PCB.

One of the most important elements of the ROV is a tether connecting a ground (surface) station with an underwater vehicle. The cable must contain supply wires, signal lines; often the pressure of a pneumatic or hydraulic system is also transmitted to the underwater vehicle via the cable. In addition, the cable must perform a load-carrying function and be strong enough to be able to lift the vehicle or cargo from the bottom.

Properties that the tether must meet:

- High tensile strength—this is necessary so that the tether can withstand the weight of the ROV and cargo;
- Neutral buoyancy—a non-floating tether will greatly affect the underwater vehicle and prevent it from performing operations;
- Interference immunity—in the case of using communication over metal conductors, protection against interference caused by supply conductors is required;
- Low resistivity of power lines—the tether length in some cases reaches several kilometers, which causes a large total resistance of the cable and leads to power losses;
- Protection against mechanical damage—protection against damage is a necessary parameter of the cable since a damaged tether can cause damage to the electronics of the vehicle or divers;
- High flexibility—a tether with low flexibility will severely limit the robot's capabilities in narrow and confined spaces;
- The ability to twist several times during operation—the ROV will often make turns and thus can damage the internal structure of the tether if it is not able to twist.

The tether used in SevROV is a custom-made product containing 8 cores for power lines, 4 signal cores, and 2 coaxial channels for video.

2.2.4. The Carrier System

According to the purposed scheme, a frame was developed for the designed ROV. The frame takes into account the peculiarities of the location of the thrusters and other elements of the vehicle.

The main purpose of designing the structure of the ROV was to compactly and reliably place and fix all the elements of the ROV on the frame with the maximum preservation of the center of mass in the vicinity of the geometric center.

The design of the ROV is not streamlined and refers to open frame structures in which all elements of the robot are attached to an open frame. The frame of the ROV is made of a polyethylene sheet and is collapsible, the method of fastening the frame elements is groove to groove. Thus, the ROV is collapsible and easy to maintain, and the issues of streamlining and hydrodynamics can be neglected due to the relatively small dimensions and low speeds of the ROV.

The 3D model of the SevROV frame is shown in Figure 5a. The frame was designed in the Fusion 360 and SolidWorks computer-aided design systems. The result of assembling a complete 3D model of SevROV is shown in Figure 5b.

(**a**) (**b**)

Figure 5. (**a**) Three-dimensional (3D) model of SevROV frame; (**b**) 3D model of assembled SevROV.

The carrier system serves to unite all components of the vehicle into a single structure and determines all dimensions and arrangements of the components. The frame provides

the layout of the thrusters and the placement of other components to achieve maximum stability of the vehicle.

The second part of the carrier system is the buoyancy elements and the ballast. Since this vehicle experimental sample is not designed for diving to depths of more than 200 m, Styrofoam was chosen for the buoyancy elements, as an additional and easily processed material with a low density.

A sealed housing has been developed for the electronics, the purpose of which is to keep a dry environment inside the vehicle and not allow water to damage the electronics.

This was provided by a series of O-rings and special sealed connectors. Moreover, the sealed case is designed with a large reserve in depth, which will allow further modifications and testing of the vehicle if necessary.

This unit must be capable of accommodating all electronic components and capable of maintaining hermeticity at a depth of 200 m. The hermetically sealed unit was also developed in CAD Fusion 360, which made it easy to create drawings for further production of the unit. The Hermetically sealed unit is shown in Figure 6a. There are no windows in the unit casing, therefore the ROV uses an external camera. On the first cap of the HSU, there are special holes for penetrators—collapsible sealed inputs for connecting external components. The second cap only has a depth gauge and a pressure relief valve/sealed check valve. The valve on the second cap is used only for ease of assembly and surface tightness testing. To ensure tightness, grooves are provided for rubber seals, this allows for tightness for depths of more than 100 m (see Figure 6b).

(**a**) (**b**)

Figure 6. (**a**) Hermetically sealed unit for electronics; (**b**) O-rings of the hermetically sealed unit.

2.3. SevROV Motion Mathematical Model

2.3.1. Kinematics Model of the SevROV

The general motion of an underwater robot in six degrees of freedom in a fixed frame associated with the body with o_b as the origin is described by the following vectors:

$$\boldsymbol{\eta} = \begin{bmatrix} \boldsymbol{p}^n_{b/n} (\text{or } \boldsymbol{p}^e_{b/n}) \\ \boldsymbol{\Theta}_{nb} \end{bmatrix}, \boldsymbol{v} = \begin{bmatrix} \boldsymbol{v}^b_{b/n} \\ \boldsymbol{\omega}_{nb} \end{bmatrix}, \boldsymbol{\tau} = \begin{bmatrix} \boldsymbol{f}^b_b \\ \boldsymbol{m}^b_b \end{bmatrix} \quad (1)$$

where $\boldsymbol{\eta} \in R^3 \times S^3$ denotes the vector of position and orientation, where the vector of position $\boldsymbol{p}^n_{b/n} \in R^3$—is the distance from NED to BODY, expressed in NED coordinates, $\boldsymbol{\Theta}_{nb} \in S^3$ is the vector of Euler angles, $\boldsymbol{v} \in R^6$ denotes vectors of linear and angular velocities, which are decomposed in a fixed frame, and $\boldsymbol{\tau} \in R^6$ is used to describe forces and moments acting on the apparatus in a stationary frame of reference (see Figure 7):

- x_b is a longitudinal axis (directed from stern to bow);
- y_b is a transverse axis (directed to the right side);
- z_b is a normal axis (directed from top to bottom).

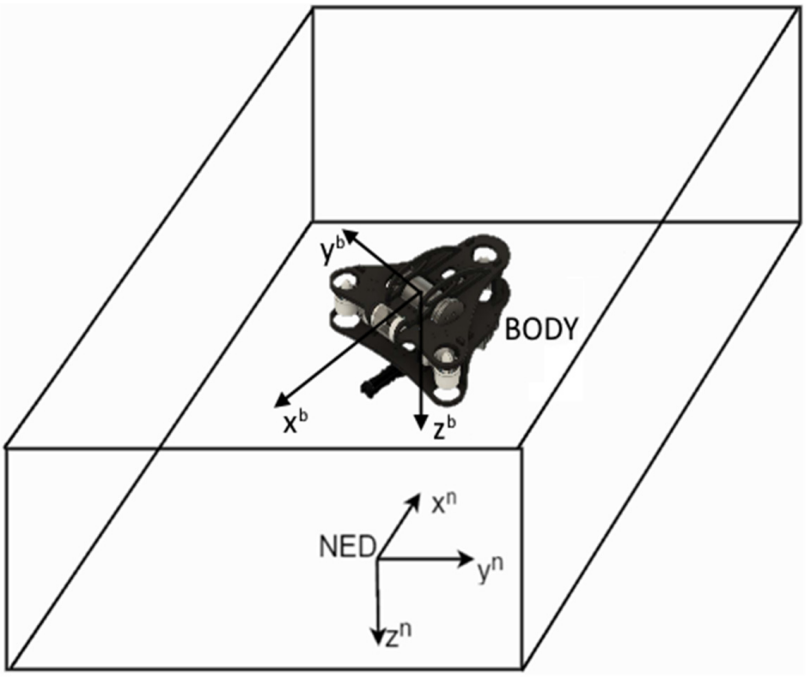

Figure 7. BODY frame (x_b, y_b, z_b) in the NED frame (x_n, y_n, z_n).

The kinematics model of the ROV in vector–matrix form has the form [17,18]

$$\begin{gathered} \dot{\boldsymbol{\eta}} = \boldsymbol{J}_{\Theta}(\boldsymbol{\eta})\boldsymbol{v} \\ \Updownarrow \\ \begin{bmatrix} \dot{\boldsymbol{p}}^{n}_{b/n} \\ \dot{\boldsymbol{\Theta}}_{nb} \end{bmatrix} = \begin{bmatrix} \boldsymbol{R}^{n}_{b}(\boldsymbol{\Theta}_{nb}) & 0_{3\times 3} \\ 0_{3\times 3} & \boldsymbol{T}_{\Theta}(\boldsymbol{\Theta}_{nb}) \end{bmatrix} \begin{bmatrix} \boldsymbol{v}^{b}_{b/n} \\ \boldsymbol{\omega}^{b}_{b/n} \end{bmatrix}. \end{gathered} \tag{2}$$

where

$$\boldsymbol{\eta} = \begin{bmatrix} \boldsymbol{p}^{n}_{b/n} \\ \boldsymbol{\Theta}_{nb} \end{bmatrix},\ \boldsymbol{v} = \begin{bmatrix} \boldsymbol{v}^{b}_{b/n} \\ \boldsymbol{\omega}^{b}_{b/n} \end{bmatrix},\ \boldsymbol{J}_{\Theta}(\boldsymbol{\eta}) = \begin{bmatrix} \boldsymbol{R}^{n}_{b}(\boldsymbol{\Theta}_{nb}) & 0_{3\times 3} \\ 0_{3\times 3} & \boldsymbol{T}_{\Theta}(\boldsymbol{\Theta}_{nb}) \end{bmatrix},$$

$$\boldsymbol{p}^{n}_{b/n} = [x_n, y_n, z_n]^T,\ \boldsymbol{\Theta}_{nb} = [\varphi,\ \theta,\ \psi]^T,\ \boldsymbol{v}^{n}_{b/n} = [u,\ v,\ w]^T,\ \boldsymbol{\omega}^{b}_{b/n} = [p,\ q,\ r]^T,$$

and matrices of rotation $\boldsymbol{R}^{n}_{b}(\Theta_{nb})$ and transformation $\boldsymbol{T}_{\Theta}(\boldsymbol{\Theta}_{nb})$ have the form

$$\begin{gathered} \boldsymbol{R}^{n}_{b}(\boldsymbol{\Theta}_{nb}) = \begin{bmatrix} c\psi c\theta & -s\psi c\varphi + c\psi s\theta s\varphi & s\psi s\varphi + c\psi c\varphi s\theta \\ s\psi c\theta & c\psi c\varphi + s\varphi s\theta s\psi & -c\psi s\varphi + s\theta s\psi c\varphi \\ -s\theta & c\theta s\varphi & c\theta c\varphi \end{bmatrix}, \\ \boldsymbol{T}^{-1}_{\Theta}(\boldsymbol{\Theta}_{nb}) = \begin{bmatrix} 1 & 0 & -s\theta \\ 0 & c\varphi & c\theta s\varphi \\ 0 & -s\varphi & c\theta c\varphi \end{bmatrix} \Rightarrow \boldsymbol{T}_{\Theta}(\boldsymbol{\Theta}_{nb}) = \begin{bmatrix} 1 & s\varphi t\theta & c\varphi t\theta \\ 0 & c\varphi & -s\varphi \\ 0 & s\varphi/c\theta & c\varphi/c\theta \end{bmatrix} \end{gathered} \tag{3}$$

where $s\bullet = \sin(\bullet)$ and $c\bullet = \cos(\bullet)$.

2.3.2. Dynamics Model of the SevROV

The dynamics model of the ROV as a rigid body is expressed as [17,18]:

$$\boldsymbol{M}\dot{\boldsymbol{v}} + \boldsymbol{C}(\boldsymbol{v})\boldsymbol{v} + \boldsymbol{D}(\boldsymbol{v})\boldsymbol{v} + \boldsymbol{g}(\boldsymbol{\eta}) = \boldsymbol{\tau}, \tag{4}$$

where

$$\boldsymbol{M} = \boldsymbol{M}_{RB} + \boldsymbol{M}_A,\ \boldsymbol{C}(\boldsymbol{v}) = \boldsymbol{C}_{RB}(\boldsymbol{v}) + \boldsymbol{C}_A(\boldsymbol{v}),$$

$$\boldsymbol{M}_{RB} = \begin{bmatrix} m & 0 & 0 & 0 & mz_g & -my_g \\ 0 & m & 0 & -mz_g & 0 & mx_g \\ 0 & 0 & m & my_g & -mx_g & 0 \\ 0 & -mz_g & my_g & I_x & -I_{xy} & -I_{xz} \\ mz_g & 0 & -mx_g & -I_{yx} & I_y & -I_{yz} \\ -my_g & mx_g & 0 & -I_{zx} & -I_{zy} & I_z \end{bmatrix}, \boldsymbol{M}_A = -\begin{bmatrix} X_{\dot{u}} & 0 & 0 & 0 & 0 & 0 \\ 0 & Y_{\dot{v}} & 0 & 0 & 0 & 0 \\ 0 & 0 & Z_{\dot{w}} & 0 & 0 & 0 \\ 0 & 0 & 0 & K_{\dot{p}} & 0 & 0 \\ 0 & 0 & 0 & 0 & M_{\dot{q}} & 0 \\ 0 & 0 & 0 & 0 & 0 & N_{\dot{r}} \end{bmatrix},$$

$$\boldsymbol{C}_{RB}(\boldsymbol{v}) = \begin{bmatrix} 0 & 0 & 0 & 0 & mw & 0 \\ 0 & 0 & 0 & -mw & 0 & 0 \\ 0 & 0 & 0 & mv & -mu & 0 \\ 0 & mw & -mv & 0 & I_z r & -I_y q \\ -mw & 0 & -mu & -I_z r & 0 & I_x p \\ mv & -mu & 0 & I_y q & I_x p & 0 \end{bmatrix}, \boldsymbol{C}_A(\boldsymbol{v}) = \begin{bmatrix} 0 & 0 & 0 & 0 & -Z_{\dot{w}} w & Y_{\dot{v}} v \\ 0 & 0 & 0 & Z_{\dot{w}} w & 0 & -X_{\dot{u}} u \\ 0 & 0 & 0 & -Y_{\dot{v}} v & X_{\dot{u}} u & 0 \\ 0 & -Z_{\dot{w}} w & Y_{\dot{v}} v & 0 & -N_{\dot{r}} r & M_{\dot{q}} q \\ Z_{\dot{w}} w & 0 & -X_{\dot{u}} u & N_{\dot{r}} r & 0 & -K_{\dot{p}} p \\ -Y_{\dot{v}} v & X_{\dot{u}} u & 0 & -M_{\dot{q}} q & K_{\dot{p}} p & 0 \end{bmatrix}, \tag{5}$$

$$\boldsymbol{D}(v) = -\begin{bmatrix} X_u + X_{|u|u}|u| & 0 & 0 & 0 & 0 & 0 \\ 0 & Y_v + Y_{|v|v}|v| & 0 & 0 & 0 & 0 \\ 0 & 0 & Z_w + Z_{|w|w}|w| & 0 & 0 & 0 \\ 0 & 0 & 0 & K_p + K_{p|p|}|p| & 0 & 0 \\ 0 & 0 & 0 & 0 & M_q + M_{q|q|}|q| & 0 \\ 0 & 0 & 0 & 0 & 0 & N_r + N_{|r|r}|r| \end{bmatrix}, \tag{6}$$

$$\boldsymbol{g}(\boldsymbol{\eta}) = \begin{bmatrix} (W - B)\sin\theta \\ -(W - B)\cos\theta\sin\varphi \\ -(W - B)\cos\theta\cos\varphi \\ -(y_g W - y_b B)\cos\theta\cos\varphi + (z_g W - z_b B)\cos\theta\sin\varphi \\ (z_g W - z_b B)\sin\theta + (x_g W - x_b B)\cos\theta\cos\varphi \\ -(x_g W - x_b B)\cos\theta\sin\varphi - (y_g W - y_b B)\sin\theta \end{bmatrix},$$

where I_x, I_y, I_z are the moments of inertia about the axes x_b, y_b, z_b, $I_{xy} = I_{yx}, I_{xz} = I_{zx}$ and $I_{yz} = I_{zy}$ are the products of inertia [17]; $r_g = [x_g\ y_g\ z_g]^T$ is the vector determines the position of the center of gravity concerning the geometric center of the vehicle; W is the force due to the gravitational attraction of the system, and B is the buoyancy force; $X_{\dot{u}}$, $Y_{\dot{v}}$, $Z_{\dot{w}}$, $K_{\dot{p}}$, $M_{\dot{q}}$, $N_{\dot{r}}$ are added masses; X_u, Y_v, Z_w, K_p, M_q, N_r are coefficients of linear damping; $X_{|u|u}$, $Y_{|v|v}$, $Z_{|w|w}$, $K_{p|p|}$, $M_{q|q|}$, $N_{|r|r}$ are the quadratic damping coefficients.

Since the origin of the BODY frame is placed in the geometric center of the vehicle, and assuming that the vehicle has symmetry in the xz plane (left and right sides) and in the xy plane, the mass matrix can be simplified by taking $x_g = y_g = 0$ and $I_{xy} = I_{xz} = I_{zy} = 0$:

$$\boldsymbol{M}_{RB} = \begin{bmatrix} m & 0 & 0 & 0 & mz_g & 0 \\ 0 & m & 0 & -mz_g & 0 & 0 \\ 0 & 0 & m & 0 & 0 & 0 \\ 0 & -mz_g & 0 & I_x & 0 & 0 \\ mz_g & 0 & 0 & 0 & I_y & 0 \\ 0 & 0 & 0 & 0 & 0 & I_z \end{bmatrix}.$$

Moreover, under the assumption that the center of the BODY frame x_b, y_b, z_b is aligned with the center of buoyancy, i.e.,$x_b = y_b = z_b = 0$, the vector of gravitational force and buoyancy force can be simplified to the form

$$g(\eta) = \begin{bmatrix} (W-B)\sin\theta \\ -(W-B)\cos\theta\sin\varphi \\ -(W-B)\cos\theta\cos\varphi \\ z_g W\cos\theta\sin\varphi \\ z_g W\sin\theta \\ 0 \end{bmatrix}.$$

The values of other parameters in (5), (6) were found based on the calculation method described in [19].

2.3.3. Thrust Configuration and Power Coefficients Matrices

It is convenient to express the forces and moments of control as [17]

$$f = Ku, \tag{7}$$

where $u = [u_1, \ldots, u_6]^T$ is a vector of control inputs; $K \in R^{6\times6}$ is a diagonal matrix of force coefficients, defined as

$$K = diag[K_1, \ldots, K_6].$$

The forces and moments of the thrusters refer to the control input as

$$\tau = T(\alpha)f = T(\alpha)Ku.$$

where $\alpha = [\alpha_1, \ldots, \alpha_6]$ is the vector of angles through which the thrusters are turned, and $T(\alpha) \in R^{6\times6}$ is the thruster's configuration matrix, describes the geometry or arrangement of the thrusters.

Given the force vector $f = [F_x,\ F_y,\ F_z]^T$ and the arms of forces $r = [l_x,\ l_y,\ l_z]^T$, forces and moments in 6 degrees of freedom can be determined as follows [17]:

$$\tau = \begin{bmatrix} f \\ r\times f \end{bmatrix}, f = \begin{bmatrix} F_x \\ F_y \\ F_z \end{bmatrix}, r\times f = \begin{bmatrix} F_x l_z - F_y l_y \\ F_x l_z - F_z l_x \\ F_y l_x - F_x l_y \end{bmatrix}. \tag{8}$$

The thruster's configuration matrix $T(\alpha)$ can then be calculated using Equation (8).

In Figure 8 a top and front view of a SevROV are shown. Accordingly, the arms of the moments of forces of 6 thrusters relative to the center of gravity (CG) are calculated and presented in Table 2.

Table 2. Moment arms of the SevROV.

Number of Thruster	l_{xi}, m	l_{yi}, m	l_{zi}, m
1	0.15125	0	−0.00387
2	0.07563	0.13099	−0.00387
3	0.07563	0.13099	−0.00387
4	0.225	0	0
5	0.1125	0.19486	0
6	0.1125	0.19486	0

The rotation angles for horizontal thrusters of 1 to 3 are $\pi/2$, $-\pi/6$, $\pi/6$, respectively, and thrusters 4 to 6 are vertical thrusters without horizontal rotations.

Subsequently, using (8) the forces and moments produced by thruster:

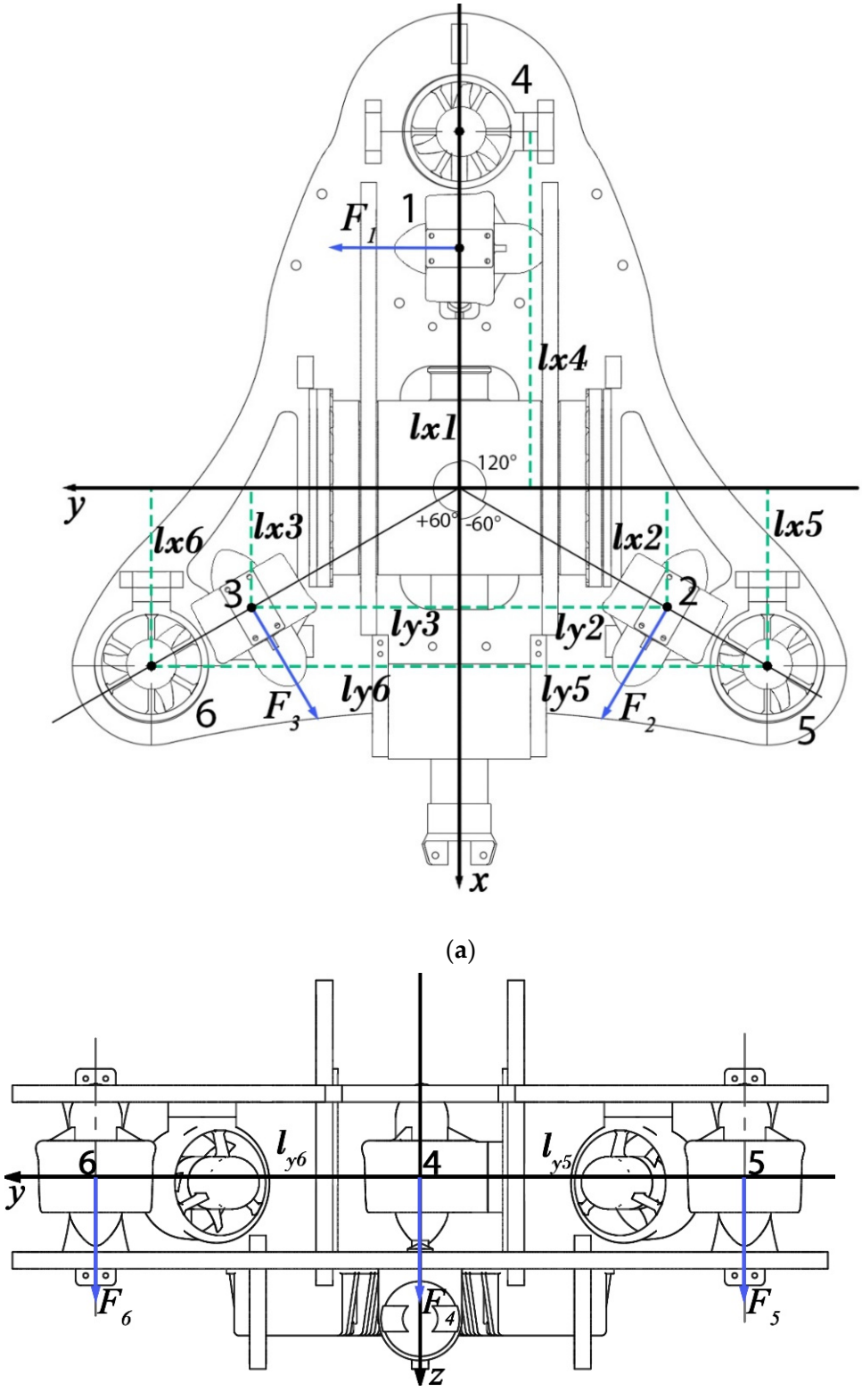

Figure 8. (**a**) Top view of the SevROV; (**b**) front view of the SevROV.

$$\boldsymbol{\tau}_1 = \begin{bmatrix} 0 \\ F_1 \\ 0 \\ F_1 l_{z1} \\ 0 \\ F_1 l_{x1} \end{bmatrix} = \begin{bmatrix} 0 \\ 1 \\ 0 \\ l_{z1} \\ 0 \\ l_{x1} \end{bmatrix} F_1,$$

$$\boldsymbol{\tau}_2 = \begin{bmatrix} F_2 \cos(\pi/6) \\ F_2 \sin(\pi/6) \\ 0 \\ F_2 \sin(\pi/6) l_{z2} \\ F_2 \cos(\pi/6) l_{z2} \\ F_2 \sin(\pi/6) l_{x2} + F_2 \cos(\pi/6) l_{y2} \end{bmatrix} = \begin{bmatrix} \cos(\pi/6) \\ \sin(\pi/6) \\ 0 \\ \sin(\pi/6) l_{z2} \\ \cos(\pi/6) l_{z2} \\ \sin(\pi/6) l_{x2} + \cos(\pi/6) l_{y2} \end{bmatrix} F_2,$$

$$\boldsymbol{\tau}_3 = \begin{bmatrix} F_3 \cos(\pi/6) \\ -F_3 \sin(\pi/6) \\ 0 \\ -F_3 \sin(\pi/6) l_{z3} \\ F_3 \cos(\pi/6) l_{z3} \\ -F_3 \sin(\pi/6) l_{x3} - F_3 \cos(\pi/6) l_{y3} \end{bmatrix} = \begin{bmatrix} \cos(\pi/6) \\ -\sin(\pi/6) \\ 0 \\ -\sin(\pi/6) l_{z3} \\ \cos(\pi/6) l_{z3} \\ -\sin(\pi/6) l_{x3} - \cos(\pi/6) \end{bmatrix} F_3, \tag{9}$$

$$\boldsymbol{\tau}_4 = \begin{bmatrix} 0 \\ 0 \\ F_4 \\ 0 \\ F_4 l_{x4} \\ 0 \end{bmatrix} = \begin{bmatrix} 0 \\ 0 \\ 1 \\ 0 \\ l_{x4} \\ 0 \end{bmatrix} F_4, \boldsymbol{\tau}_5 = \begin{bmatrix} 0 \\ 0 \\ F_5 \\ -F_5 l_{y5} \\ -F_5 l_{x5} \\ 0 \end{bmatrix} = \begin{bmatrix} 0 \\ 0 \\ 1 \\ -l_{y5} \\ -l_{x5} \\ 0 \end{bmatrix} F_5, \boldsymbol{\tau}_6 = \begin{bmatrix} 0 \\ 0 \\ F_6 \\ F_6 l_{y6} \\ -F_6 l_{x6} \\ 0 \end{bmatrix} = \begin{bmatrix} 0 \\ 0 \\ 1 \\ l_{y6} \\ -l_{x6} \\ 0 \end{bmatrix} F_6.$$

As a result, from (9), the matrix of the thruster's configuration created by a total of six thrusters will be equal to:

$$\boldsymbol{T}(\boldsymbol{\alpha}) = \begin{bmatrix} 0 & 0.866 & 0.866 & 0 & 0 & 0 \\ 1 & 0.5 & -0.5 & 0 & 0 & 0 \\ 0 & 0 & 0 & 1 & 1 & 1 \\ l_{z1} & 0.5 l_{z2} & -0.5 l_{z3} & 0 & -l_{y5} & l_{y6} \\ 0 & 0.866 l_{z2} & 0.866 l_{z3} & l_{x4} & -l_{x5} & -l_{x6} \\ l_{x1} & 0.5 l_{x2} + 0.866 l_{y2} & -0.5 l_{x3} - 0.866 l_{y3} & 0 & 0 & 0 \end{bmatrix}.$$

Knowing the distribution of forces and moments, the control input $\boldsymbol{u}$ can be calculated to be applied to the motors in such a way that the desired control can be generalized forces $\boldsymbol{\tau}$. Since the control forces and moments caused by the thrusters relative to the control inputs are expressed through (7), the vector of control inputs can be obtained in the form:

$$\boldsymbol{u} = \boldsymbol{K}^{-1} \boldsymbol{T}(\boldsymbol{\alpha})^{-1} \boldsymbol{\tau}. \tag{10}$$

An important nuance is that due to the proposed design and thruster's arrangement, the configuration matrix $\boldsymbol{T}(\boldsymbol{\alpha})$ is square and non-degenerate, which allows not to resort to pseudo-inversion in the expression (10) for calculating the control.

3. Results

As a result, an underwater vehicle SevROV of inspection class with a Y-shaped arrangement of the thrusters was proposed, which allowed using six thrusters to obtain the controllability of the vehicle by six degrees of freedom. The appearance of the manufactured experimental sample SevROV is shown in Figure 9. To achieve zero buoyancy of the robot, buoyancy elements made of extruded polystyrene foam were added to its frame.

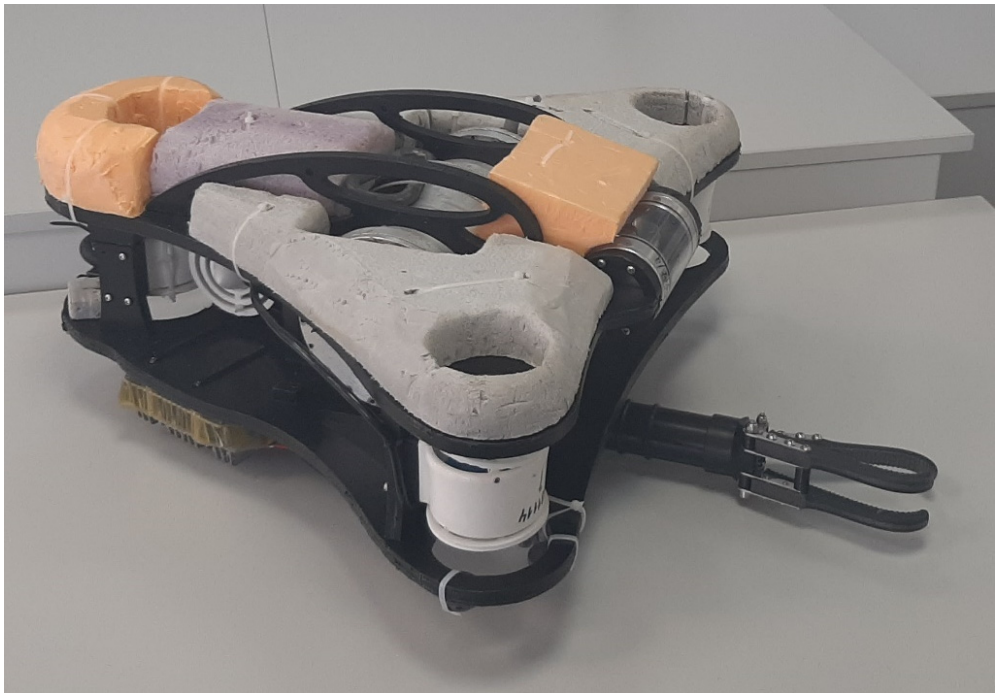

Figure 9. The appearance of the experimental sample SevROV.

To stabilize the robot's movement and realize in the future the possibility of complex trajectory movement in automatic mode, a mathematical model of the robot was developed and its parameters were identified. The description of the model is presented in Section 2.3. This model was implemented in the MATLAB & Simulink system. A computer simulation of the developed model was performed and compared with real experiments, which confirmed the adequacy of the model. The simulation and experimental tests results are presented below.

Results of Modeling and Testing of Experimental ROV

The initial tests of the SevROV were carried out in a large experimental aquarium. Aquarium parameters: length—3.35 m, width—2.4 m, height—2.2 m. An onboard navigation system based on the NavX 2 module, a depth sensor, and external observation and measurement devices were used as a means of measuring the parameters of the SevROV movement.

NavX 2 inertial navigation module provided data on angular displacements for roll, pitch, and yaw. Since the accuracy of linear displacement measurements based on the NavX2 had a large cumulative error (1 m in 15 s), external measurement instruments based on the stereo vision module were used to determine the linear displacements and coordinates of the vehicle. This module was developed earlier within the framework of another project. The stereo vision module was designed to search for and determine the coordinates of objects in the workspace of an underwater robot [20,21]. The accuracy of determining the coordinates of an object using the stereo vision module was: 0.5 mm for the horizontal and vertical coordinates of the image; 7.5 mm for the distance to the object (image depth) [22]. The external view of the equipment and the layout are shown in Figure 10. An example of measuring SevROV coordinates using the stereo vision module is shown in Figure 11.

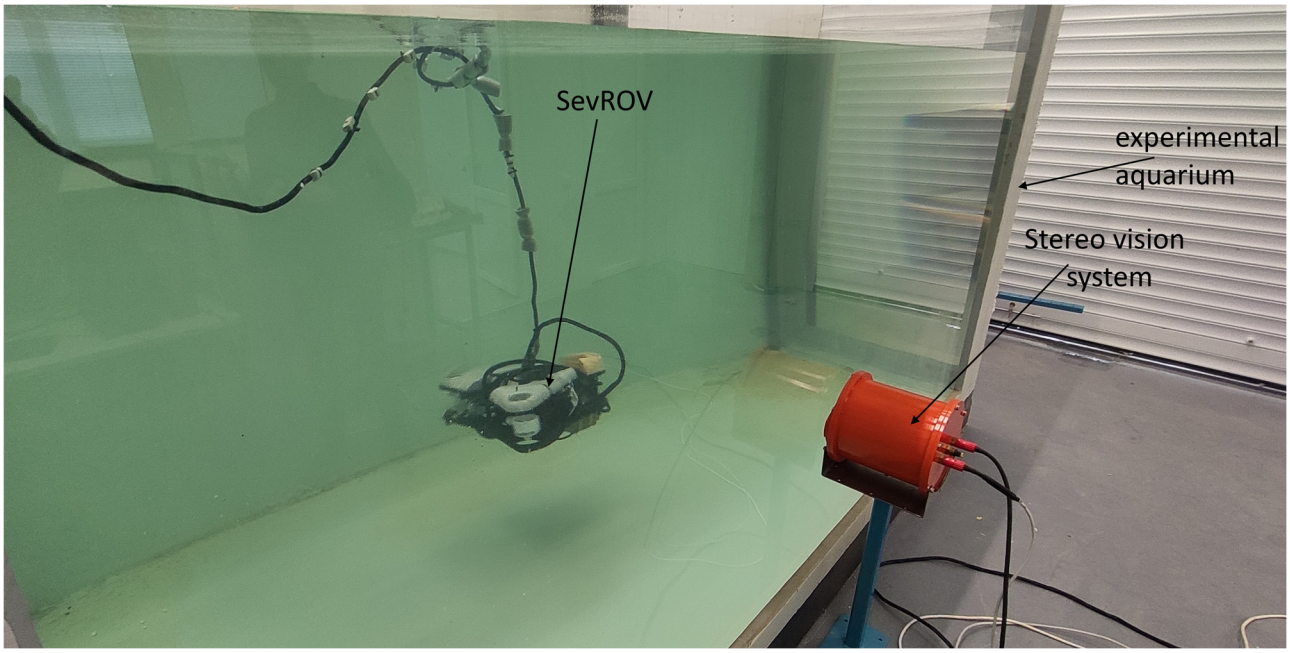

Figure 10. The appearance of the equipment and the layout.

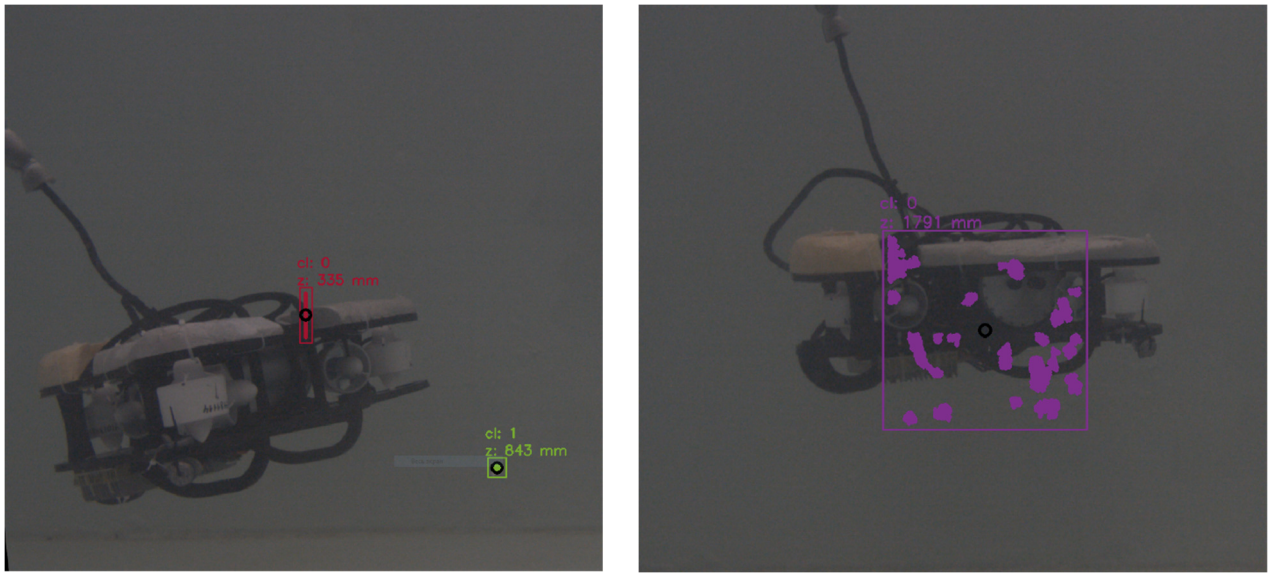

Figure 11. Example of SevROV position measurement using stereo vision module.

The first experiment: the robot was located at the origin of the NED frame; it was necessary to first apply a control action to perform a set of movements corresponding to each linear movement degree of freedom sequentially (up–down, forward–backward, left–right consistently), then perform combined motions (backward, up, and right).

The second experiment: the robot was located at the origin of the NED frame; it was necessary to first apply a control action to perform a vertical movement to a certain depth, and then sequentially perform a set of movements corresponding to each angular movement degree of freedom sequentially (yaw, pitch, and roll).

The control parameters $\boldsymbol{u}$ were calculated from (10), and the values of the vector of forces and moments were taken as shown in Table 3.

Table 3. Vector of forces and moments, control vector of the SevROV.

Type of Movement	Vector of Forces and Moments, τ
The first experiment	
Dive	$\tau = [\ 0 \quad 0 \quad -44.13 \quad 0 \quad 0 \quad 0\ ]^T$
Forward	$\tau = [\ 25.49 \quad 0 \quad 0 \quad 0 \quad 0 \quad 0\ ]^T$
To the left	$\tau = [\ 0 \quad -33.34 \quad 0 \quad 0 \quad 0 \quad 0\ ]^T$
Backward, up, and right	$\tau = [\ -25.49 \quad 33.34 \quad -44.13 \quad 0 \quad 0 \quad 0\ ]^T$
The second experiment	
Clockwise yaw	$\tau = [\ 0 \quad 0 \quad 0 \quad 6.67 \quad 0 \quad 0\ ]^T$
Counterclockwise yaw	$\tau = [\ 0 \quad 0 \quad 0 \quad -6.67 \quad 0 \quad 0\ ]^T$
Clockwise pitch	$\tau = [\ 0 \quad 0 \quad 0 \quad 0 \quad 5.92 \quad 0\ ]^T$
Counterclockwise pitch	$\tau = [\ 0 \quad 0 \quad 0 \quad 0 \quad -5.92 \quad 0\ ]^T$
Clockwise roll	$\tau = [\ 0 \quad 0 \quad 0 \quad 0 \quad 0 \quad 5.16\ ]^T$
Counterclockwise roll	$\tau = [\ 0 \quad 0 \quad 0 \quad 0 \quad 0 \quad -5.16\ ]^T$

The results of the modeling and experimental tests for both experiments are presented in Figures 12 and 13. For the first experiment (Figure 12), the simulated trajectory of the SevROV is presented by the solid line, the real trajectory of the SevROV—by dotted line. For the second experiment (Figure 13), the simulated angular motion of the SevROV is presented by the solid line, the real angular motion of the SevROV—by dotted line.

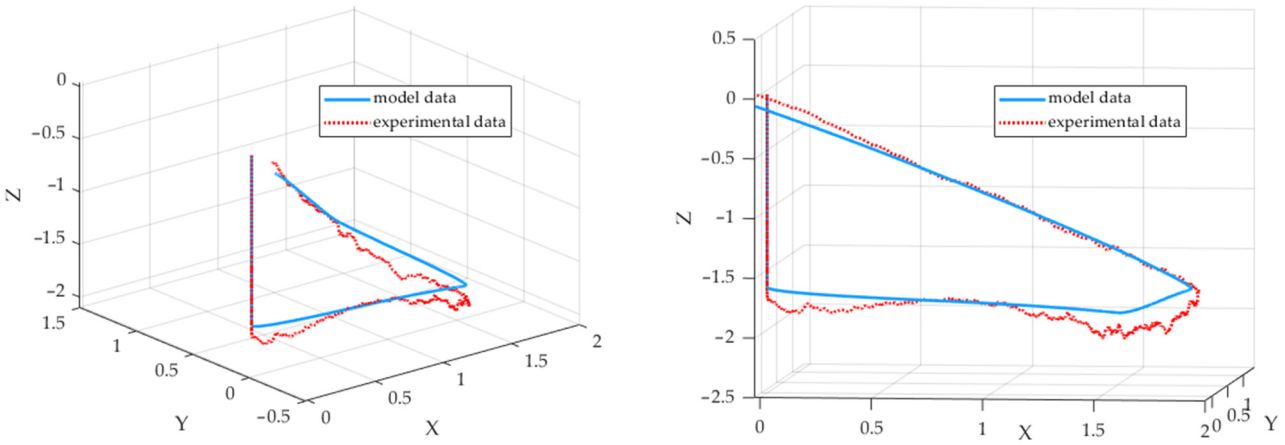

Figure 12. The first experimental results.

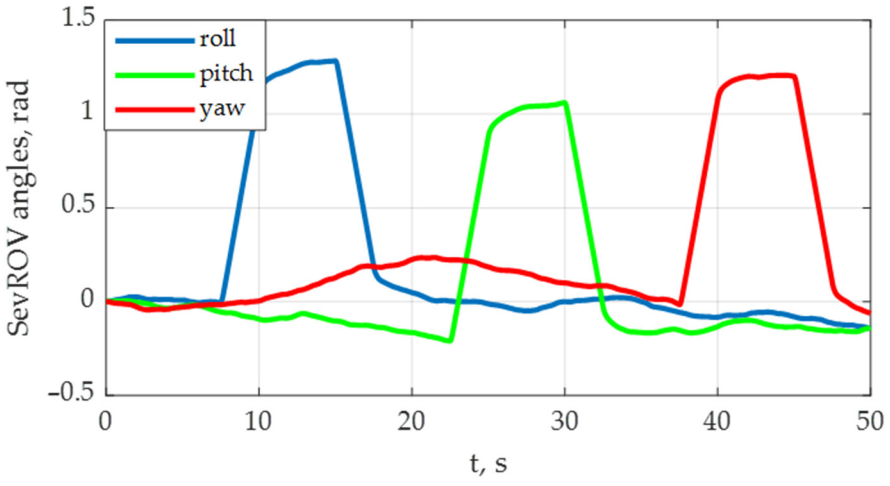

Figure 13. The second experiment results.

It can be seen from the results that the SevROV works out the given movements. The trajectory of the SevROV is close to the modeled one; however, there are noticeable errors in the measurement of inertial sensors and inaccuracies in the operation of the course stabilization regulators. In the second experiment, noises from the navigation and angular stabilization system were noticed, which are shown on the SevROV angles graph.

The SevROV sample was presented at a number of exhibitions and competitions in underwater robotics, including international competitions MATE 2021 in telepresence mode. As additional material demonstrating the SevROV, readers can get acquainted with the video at this link: https://youtu.be/dO5w4mzHYfU (accessed on 1 October 2021).

4. Discussion

The proposed design implements six degrees of freedom of the ROV with six thrusters and provides energy efficiency due to the smaller number of engines compared to standard designs. To complete the work, it is necessary to develop automatic control algorithms for performing basic operations in the automatic mode. These include automatic movement along a given trajectory, stabilization of the ROV during the manipulations for moving loads, and dynamic positioning of the ROV in the working area. The problem of control law design is solved as a synergy of hardware and algorithmic software solutions.

This problem is widely covered in various sources. In particular, it should be noted that the work conducted in [23], and the references in it, are useful on this topic. In our opinion, one should consider the underwater vehicle as a hybrid, combining the properties of AUV and ROV [24]. At the same time, in our opinion, it is promising to design the control based on the forecast of critical situations [25], allowing to increase the functional stability and reliability of the system through the implementation of logical–dynamic control.

A separate task in the control system design for the SevROV is the choice of sensors. Based on the experience of the development team, we see the effective use of 3D computer vision as a target designation system for an underwater vehicle when it performs technological and inspection missions.

Author Contributions: Conceptualization, A.K. and V.K.; methodology, A.K. and V.K.; software, I.E.; validation, V.K. and I.E.; formal analysis, V.K.; investigation, A.K., V.K. and I.E.; resources, A.K.; writing—original draft preparation, A.K. and I.E.; writing—review and editing, V.K.; visualization, I.E.; supervision, A.K.; project administration, A.K.; funding acquisition, A.K. All authors have read and agreed to the published version of the manuscript.

Funding: The research is supported by the Ministry of Science and Higher Education of the Russian Federation in the framework of the basic part of the state order № 075-03-2021-092/5 from 29.09.2021.

Institutional Review Board Statement: Not applicable.

Informed Consent Statement: Not applicable.

Data Availability Statement: The data presented in this study are available on request from the corresponding author.

Conflicts of Interest: The authors declare no conflict of interest.

References

1. Zereik, E.; Bibuli, M.; Mišković, N.; Ridao, P.; Pascoal, A. Challenges and Future Trends in Marine Robotics. *Annu. Rev. Control* **2018**, *46*, 350–368. [CrossRef]
2. Neira, J.; Sequeiros, C.; Huamani, R.; Machaca, E.; Fonseca, P.; Nina, W. Review on Unmanned Underwater Robotics, Structure Designs, Materials, Sensors, Actuators, and Navigation Control. *J. Robot.* **2021**, *2021*, 1–26. [CrossRef]
3. He, Y.; Wang, D.B.; Ali, Z.A. A Review of Different Designs and Control Models of Remotely Operated Underwater Vehicle. *Meas. Control* **2020**, *53*, 1561–1570. [CrossRef]
4. Aguzzi, J.; Costa, C.; Calisti, M.; Funari, V.; Stefanni, S.; Danovaro, R.; Gomes, H.; Vecchi, F.; Dartnell, L.; Weiss, P.; et al. Research Trends and Future Perspectives in Marine Biomimicking Robotics. *Sensors* **2021**, *21*, 3778. [CrossRef] [PubMed]

5. Abdullah, A.M.; Zakaria, N.I.; Jalil, K.A.A.; Othman, N.; Dahalan, W.M.; Hamid, H.; Ghani, M.F.; Haidir, A.Y.I.b.M.; Kamro, M.I.M. Review of the Control System for an Unmanned Underwater Remotely Operated Vehicle. In *Engineering Applications for New Materials and Technologies*; Öchsner, A., Ed.; Advanced Structured Materials; Springer International Publishing: Cham, Switzerland, 2018; Volume 85, pp. 609–631. [CrossRef]
6. Kumar, S.; Rastogi, V.; Gupta, P. Recent Developments in Modeling and Control of Underwater Robot Manipulator: A Review. *Indian J. Sci. Technol.* **2016**, *9*. [CrossRef]
7. Terracciano, D.S.; Bazzarello, L.; Caiti, A.; Costanzi, R.; Manzari, V. Marine Robots for Underwater Surveillance. *Curr. Robot. Rep.* **2020**, *1*, 159–167. [CrossRef]
8. Antonelli, G.; Fossen, T.I.; Yoerger, D.R. Modeling and Control of Underwater Robots. In *Springer Handbook of Robotics*; Siciliano, B., Khatib, O., Eds.; Springer International Publishing: Cham, Switzerland, 2016; pp. 1285–1306. [CrossRef]
9. Capocci, R.; Dooly, G.; Omerdić, E.; Coleman, J.; Newe, T.; Toal, D. Inspection-Class Remotely Operated Vehicles—A Review. *J. Mar. Sci. Eng.* **2017**, *5*, 13. [CrossRef]
10. Aguirre-Castro, O.A.; Inzunza-González, E.; García-Guerrero, E.E.; Tlelo-Cuautle, E.; López-Bonilla, O.R.; Olguín-Tiznado, J.E.; Cárdenas-Valdez, J.R. Design and Construction of an ROV for Underwater Exploration. *Sensors* **2019**, *19*, 5387. [CrossRef] [PubMed]
11. Karras, G.C.; Bechlioulis, C.P.; Abdella, H.K.; Larkworthy, T.; Kyriakopoulos, K.; Lane, D. A Robust Sonar Servo Control Scheme for Wall-Following Using an Autonomous Underwater Vehicle. In Proceedings of the 2013 IEEE/RSJ International Conference on Intelligent Robots and Systems, Tokyo, Japan, 3–7 November 2013; IEEE: Tokyo, Japan, 2013; pp. 3893–3898. [CrossRef]
12. Lin, X.; Guo, S. Development of a Spherical Underwater Robot Equipped with Multiple Vectored Water-Jet-Based Thrusters. *J. Intell. Robot. Syst.* **2012**, *67*, 307–321. [CrossRef]
13. Yue, C.; Guo, S.; Shi, L. Hydrodynamic Analysis of the Spherical Underwater Robot SUR-II. *Int. J. Adv. Robot. Syst.* **2013**, *10*, 247. [CrossRef]
14. Li, Y.; Guo, S.; Wang, Y. Design and Characteristics Evaluation of a Novel Spherical Underwater Robot. *Robot. Auton. Syst.* **2017**, *94*, 61–74. [CrossRef]
15. Yang, R.; Clement, B.; Mansour, A.; Li, M.; Wu, N. Modeling of a Complex-Shaped Underwater Vehicle for Robust Control Scheme. *J. Intell. Robot. Syst.* **2015**, *80*, 491–506. [CrossRef]
16. Li, Q.; Cao, Y.; Li, B.; Ingram, D.M.; Kiprakis, A. Numerical Modelling and Experimental Testing of the Hydrodynamic Characteristics for an Open-Frame Remotely Operated Vehicle. *J. Mar. Sci. Eng.* **2020**, *8*, 688. [CrossRef]
17. Fossen, T.I. *Handbook of Marine Craft Hydrodynamics and Motion Control*; John Wiley & Sons, Ltd.: Chichester, UK, 2014.
18. Antonelli, G. *Underwater Robots*; Springer Tracts in Advanced Robotics; Springer International Publishing: Cham, Switzerland, 2014; Volume 96. [CrossRef]
19. Eidsvik, O.A.; Schjølberg, I. Determination of Hydrodynamic Parameters for Remotely Operated Vehicles. In *Volume 7: Ocean Engineering*; American Society of Mechanical Engineers: Busan, Korea, 2016; p. V007T06A025. [CrossRef]
20. Kramar, V.; Kabanov, A.; Kramar, O.; Putin, A. Modeling and Testing of Control System for an Underwater Dual-Arm Robot. *IOP Conf. Ser. Mater. Sci. Eng.* **2020**, *971*, 042076. [CrossRef]
21. Kramar, V.; Alchakov, V.V. The Methodology of Training an Underwater Robot Control System for Operator Actions. *J. Phys. Conf. Ser.* **2020**, *1661*, 012116. [CrossRef]
22. Skorohod, B.A.; Statsenko, A.V.; Fateev, S.I.; Zhilyakov, P.V. Accuracy Analysis of 3D Points Reconstructed from Workspace of Underwater Robot. *J. Phys. Conf. Ser.* **2020**, *1661*, 012124. [CrossRef]
23. Refsnes, J.E.G. Nonlinear Model-Based Control of Slender Body AUVs. Ph.D. Thesis, Norwegian University of Science and Technology, Trondheim, Norway, 2008.
24. Sørensen, A.J.; Refsnes, J. Towards Supervisory-Switched Control of Hybrid Underwater Vehicles. *Underw. Technol. Int. J. Soc. Tech.* **2009**, *28*, 141–150. [CrossRef]
25. Kabanov, A.A.; Dubovik, S.A. Methods of Modeling and Probabilistic Analysis of Large Deviations of Dynamic Systems. *J. Phys. Conf. Ser.* **2020**, *1661*, 012044. [CrossRef]